

Elevated growth temperatures alter hydraulic characteristics in trembling aspen (*Populus tremuloides*) seedlings: implications for tree drought tolerance

DANIELLE A. WAY^{1,2,*}, JEAN-CHRISTOPHE DOMEQ^{2,3} & ROBERT B. JACKSON^{1,2}

¹Department of Biology and ²Nicholas School of the Environment, Box 90328, Duke University, Durham, NC 27708, USA and ³University of Bordeaux, Bordeaux Sciences AGRO, UMR 1220 TCEM INRA, 1 Cours du général de Gaulle, 33175 Gradignan Cedex, France

ABSTRACT

Although climate change will alter both soil water availability and evaporative demand, our understanding of how future climate conditions will alter tree hydraulic architecture is limited. Here, we demonstrate that growth at elevated temperatures (ambient +5 °C) affects hydraulic traits in seedlings of the deciduous boreal tree species *Populus tremuloides*, with the strength of the effect varying with the plant organ studied. Temperature altered the partitioning of hydraulic resistance, with greater resistance attributed to stems and less to roots in warm-grown seedlings ($P < 0.02$), and a 46% (but marginally significant, $P = 0.08$) increase in whole plant conductance at elevated temperature. Vulnerability to cavitation was greater in leaves grown at high than at ambient temperatures, but vulnerability in stems was similar between treatments. A soil–plant–atmosphere (SPA) model suggests that these coordinated changes in hydraulic physiology would lead to more frequent drought stress and reduced water-use efficiency in aspen that develop at warmer temperatures. Tissue-specific trade-offs in hydraulic traits in response to high growth temperatures would be difficult to detect when relying solely on whole plant measurements, but may have large-scale ecological implications for plant water use, carbon cycling and, possibly, plant drought survival.

Key-words: cavitation vulnerability; climate change; embolism; poplar; transpiration; water; xylem.

INTRODUCTION

Evidence that the earth is warming is unequivocal. The first decade of the 21st century was the warmest on record, and high-latitude air temperatures are expected to increase between 2.5 and 6.5 °C by 2100 (Christensen *et al.* 2007). Climate change is projected to increase air temperatures

Correspondence: D. A. Way. Fax: +1 919 613 8741; e-mail: danielle.way@duke.edu

*Current address: Department of Biology, University of Western Ontario, London, ON, Canada.

and to make droughts more frequent and severe (Christensen *et al.* 2007). Because the water-holding capacity of the atmosphere increases with higher temperatures, and relative humidity is not projected to change markedly (Trenberth, Fasullo & Smith 2005), this rise in temperature will lead to a higher vapour pressure deficit (D) and increased evaporative demand and transpiration rates. However, while many studies have examined the impact of elevated growth temperatures on plant growth and CO₂ fluxes, few have quantified the effects on hydraulic properties (see review in Way & Oren 2010), even though the ability to supply water to leaves determines plant growth, productivity and survival (Meinzer 2002; Domeq *et al.* 2009).

The few studies that have examined hydraulic changes in response to growth temperature have found conflicting results. In a field gradient study on *Pinus ponderosa*, mature trees growing in warm, arid desert sites had larger tracheid diameters and higher specific hydraulic conductivity than cooler, moister montane pines (Maherali & DeLucia 2000a). Seedlings of the same species grown in chambers at elevated temperatures, but where D was allowed to vary, had similar changes in xylem anatomy and function compared to cool-grown seedlings (Maherali & DeLucia 2000b). In contrast, Thomas, Montagu & Conroy (2004) found that *Eucalyptus camaldulensis* seedlings grown at elevated temperatures (up to 37 °C) produced smaller diameter xylem vessels and had lower hydraulic conductivity than seedlings from lower growth temperatures (20–25 °C) when D was held constant between treatments. And in a recent paper, there was no consistent difference in leaf-specific hydraulic conductance of entire seedlings in either *E. saligna* or *E. sideroxylon* grown at ambient temperatures (AT) or a 4 °C warming treatment, across subambient, ambient or elevated CO₂ conditions where D varied with temperature (Phillips *et al.* 2011). Thus, the effect of growth temperature on tree water transport capacity may be positive, neutral or negative, and we know very little about whether this variety of responses is due to differences in growth conditions, such as D , species attributes or experimental approaches, such as measuring aboveground compared to whole-plant responses.

The soil–plant–atmosphere hydraulic continuum model predicts that increases in transpiring leaf area require proportional increases in xylem tissue, or xylem hydraulic capacity, to prevent catastrophic hydraulic failure when E is high (Tyree and Sperry 1988; Sperry *et al.* 1998). The need to balance the trade-off between carbon allocation to leaves (to maintain photosynthesis) versus stems and roots (to maintain E below critical levels) has led to a common plant hydraulic architecture that approaches the theoretical limit of catastrophic xylem dysfunction (Givnish 1986; Tyree and Sperry 1988). However, we have little information on how tree species may shift biomass allocation or hydraulic capacity to accomplish this trade-off under warmer conditions, despite the importance of hydraulic characteristics for tree and whole forest die-offs as the climate warms (Anderegg *et al.* 2012). Elevated growth temperatures often increase tree growth and the proportion of leaf mass in trees, with a concomitant reduction in root mass allocation (Way & Oren 2010). This developmental shift should necessitate increased water transport capacity in leaves, stems and roots from warm-grown trees to match the greater potential transpirational demand. But since roots experience less warming than aboveground plant parts as short-term air temperatures increase, root hydraulic traits may be less responsive to warming than stem and leaf hydraulic capacity.

Here, we report a novel plant response to elevated temperature, which suggests that temperature acclimation produces offsetting changes in plant hydraulic architecture in different plant organs. We grew well-irrigated *Populus tremuloides* seedlings at either ambient temperatures (AT, based on field conditions) or high temperatures (HT, ambient +5 °C), and quantified changes in growth, hydraulic properties and photosynthetic traits. We then investigated the potential impact of measured changes in these traits on carbon and water cycling with a modelling approach. This study asked four questions:

- 1 Do high growth temperatures increase seedling growth and alter biomass allocation?
- 2 Does growth at elevated temperatures increase seedling hydraulic capacity?
- 3 Are the effects of high growth temperatures on seedling water transport capacity greater in aboveground tissues than in roots?
- 4 When the physiological measurements from seedlings are scaled up, how do elevated growth temperatures affect modelled aspen water use and gross primary productivity (GPP)?

METHODS

P. tremuloides seeds (from Chalk River, ON, Canada, 46°05'N, 77°52'W, ID#9230004 in the Canadian National Tree Seed Centre) were placed in 10 × 10 × 36 cm pots filled with Fafard 52 soil mix (Conrad Fafard Inc., Agawam, MA, USA) and topped with a 2 cm layer of Athenix germination mix to facilitate germination on 16 August 2010. Seeds were

germinated in one of four growth chambers (Model M-13, Environmental Growth Chambers, Chagrin Falls, OH, USA): two ambient-temperature chambers (AT, initially 14:4 °C day:night temperatures) and two high-temperature chambers (HT, initially 19:9 °C day:night temperatures), each holding 80 pots. Seeds germinated on 21 August 2010, and all chambers provided 500 $\mu\text{mol m}^{-2} \text{s}^{-1}$ photosynthetic photon flux density (PPFD) at the soil surface provided by parallel sets of metal halide lamps and incandescent bulbs. Pots were misted thrice daily to maintain a moist surface. Two weeks after seeds germinated, seedlings were fertilized with half-strength Hoagland's solution. Four weeks after germination, light levels were increased to 1000 $\mu\text{mol m}^{-2} \text{s}^{-1}$ PPFD and twice-weekly fertilizations were added to the watering regime. While seeds germinated well in both treatments, establishment of seedlings was low [since aspen normally depends more heavily on clonal propagation (Perala 1990)], resulting in 28–30 seedlings in each AT chamber and 34–37 in each HT chamber.

Photoperiod and chamber temperature were changed weekly after germination occurred to mimic seasonal changes in day length and air temperature in the native *P. tremuloides* habitat. The AT temperatures and photoperiod were based on a 9-year average (1997–2005) from the 'Old Aspen' eddy covariance flux tower (CAOAS) in Saskatchewan, Canada (53.63N, 106.20W, 600 m a.s.l.; Table 1). The experimental growing season length was dictated by the ability of the growth chambers to maintain low AT night temperatures, and thus corresponded to field conditions from 12 May to 21 September, when night temperatures reached 4 °C. The HT treatment consisted of the same photoperiod, but with 5 °C warmer day and night temperatures than the ambient treatment. The chambers did not control humidity, so the HT treatment exposed trees to a higher D , a realistic scenario for future climates where warming is expected to occur with a constant relative humidity, and thus a higher D (Kumagai *et al.* 2004). The D varied with chamber temperature as the growing season progressed: maximum daytime D ranged from 1.01 to 2.13 kPa in the AT chambers and from 1.49 to 3.34 kPa in the HT chambers.

Growth

Shoot height was measured to the nearest 0.5 cm with a ruler and stem diameter was measured at soil level with digital calipers 15 weeks after germination. Five seedlings from each chamber were harvested at the end of the experiment (20 weeks after germination), divided into leaves, stems and roots, and dried at 70 °C for 48 h to assess dry mass. These data were combined with those from additional seedlings measured for hydraulic conductance (see below), for a sample size of eight or nine seedlings per chamber (16–17 seedlings per treatment).

Hydraulics

Hydraulic traits were assessed in the last week of the experiment (19 weeks after germination; see Table 1).

Week	AT		HT		Photoperiod (h)	PPFD ($\mu\text{mol m}^{-2} \text{s}^{-1}$)
	T_{day} ($^{\circ}\text{C}$)	T_{night} ($^{\circ}\text{C}$)	T_{day} ($^{\circ}\text{C}$)	T_{night} ($^{\circ}\text{C}$)		
1	14	4	19	9	15.6	500
2	16	5	21	10	16	500
3	17.5	6.5	22.5	11.5	16.3	500
4	18	7	23	12	16.5	500
5	18.5	7.5	23.5	12.5	16.7	1000
6	20	9	25	14	16.8	1000
7	20.5	9.5	25.5	14.5	16.8	1000
8	21	10	26	15	16.7	1000
9	23.5	12.5	28.5	17.5	16.5	1000
10	24	13	29	18	16.3	1000
11	23.5	12.5	28.5	17.5	16	1000
12	22.5	11.5	27.5	16.5	15.6	1000
13	22	11	27	16	15.2	1000
14	21	10	26	15	14.8	1000
15	20	9	25	14	14.3	1000
16	19	8	24	13	13.9	1000
17	18	7	23	12	13.4	1000
18	16	5	21	10	12.9	1000
19	15	4	20	9	12.4	1000

Table 1. Growth conditions for poplar seedlings grown under ambient (AT) or high temperatures (HT, AT +5 $^{\circ}\text{C}$)

Week, weeks after germination; T_{day} , day temperature; T_{night} , night temperature; PPFD, photosynthetic photon flux density.

Pre-dawn leaf water potential (Ψ) and mid-day leaf and stem Ψ were measured on three seedlings per chamber (six seedlings per treatment) with a Scholander pressure chamber (model 1000, PMS Instrument Company, Albany, OR, USA). Pre-dawn measurements were taken 1 h before chamber lights came on; because seedlings were watered three times daily, mid-day measurements were made in the afternoon, at least 3 h after the noon watering, but before the evening water application. Pre-dawn and mid-day leaf Ψ were measured on fully expanded, mature leaves. Mid-day stem Ψ was estimated on leaves covered with aluminium foil to prevent transpiration and thus provide an estimate of the water potential in the xylem of the stem (Meinzer 2002).

Maximum hydraulic conductance was assessed with a high-pressure flow meter (HPFM, Dynamax Inc., Houston, TX, USA) on three seedlings per chamber. The HPFM measures resistance (the inverse of conductance) as the force required to push water through a sample for a given flow rate. Seedlings were cut 5 cm above soil level and the shoot was submerged under water to stop transpiration and minimize temperature fluctuations. The intact shoot was recut under water and connected to the flow meter using compression couplings. Following the methodology prescribed by Sack *et al.* (2002) and Tyree *et al.* (2005), shoots were illuminated at a photosynthetically active radiation of 850–900 $\mu\text{mol m}^{-2} \text{s}^{-1}$. However, confirming the recent report by Voicu & Zwiazek (2010), this poplar species did not show any significant response in hydraulic conductance to irradiance when light intensity was varied. During exposure to high irradiance, the temperature of the water bath, where leaves were, increased by up to 0.7 $^{\circ}\text{C}$, so slight corrections (<2.4%) were performed to account for the

temperature-induced change in water viscosity between samples. Because seedling size differed between treatments, we measured not only whole seedling hydraulic conductance (in $\text{mmol s}^{-1} \text{MPa}^{-1}$), but also the hydraulic characteristics of a developmentally similar section of the main stem, consisting of the 12 youngest leaves. After measuring whole stem leaf-specific hydraulic conductance ($K_{\text{tree-top}}$, in $\text{mmol m}^{-2} \text{s}^{-1} \text{MPa}^{-1}$), the 12 uppermost leaves were cut off with fresh razor blades with the shoot still connected to the HPFM, then leaf laminae were cut off, then the upper 12 petioles, and finally the stem section corresponding to the top 12 leaves. After each cutting, we remeasured hydraulic conductance once the flow restabilized (typically within 3–5 min). By subtracting each measurement from the previous one, we determined the resistance explained by each plant part as it was removed (Tyree *et al.* 1993). Leaf lamina hydraulic conductance (K_{lam}) was expressed on a leaf area basis (Sack *et al.* 2002). Petiole-specific hydraulic conductivity ($k_{\text{s-petiole}}$, in $\text{kg m}^{-1} \text{s}^{-1} \text{MPa}^{-1}$) was calculated by multiplying petiole hydraulic conductance by petiole length and dividing by petiole cross-sectional area. Hydraulic resistance of the whole root system was measured by cutting the stem 2 cm above the soil and attaching the HPFM to the stem base.

Total shoot length, the length of the upper stem section (where the upper 12 leaves grew) and all 12 petioles were measured with a ruler; basal stem diameter of the whole shoot (both with and without bark), stem diameter of the base of the upper stem section and the diameter of the base of the sixth petiole (as an average of petiole diameter) were measured with digital calipers. The lower stem section was retained for measuring stem vulnerability to cavitation (see below). Leaves were separated into the 12 youngest leaves,

lower stem leaves and any leaves that were not attached to the stem during hydraulic measurements (i.e. occasional leaves near the plant base that were removed in order to attach the tubing). Leaf area of fresh leaves for each of these categories was measured with a leaf area meter (Li-Cor LI-3100C, Li-Cor, Lincoln, NE, USA); leaves were then dried to a constant mass at 70 °C and weighed. Roots were washed clean of soil and the projected area of a subsample of fine roots (<2 mm in diameter) from each seedling was measured on the leaf area meter (Li-Cor LI-3100C, Li-Cor) to estimate specific root mass; both the fine root subsample and the rest of the root were then dried at 70 °C and weighed separately for dry mass. Specific root area was estimated as the dry mass of the fine root subsample divided by the projected root area of that subsample.

Basal stem sections from the K_{plant} measurements were retained in sealed plastic bags in a refrigerator before measuring vulnerability to embolism. The segments were first used to calculate maximum stem-specific conductivity ($k_{s\text{-max}}$), calculated as the mass flow rate of the perfusion solution divided by the pressure gradient across the segment, normalized by the xylem cross-sectional area. Removal of residual air emboli was achieved by soaking samples under vacuum for 48 h with filtered water at a tension of 95 kPa. The same segments were then used to estimate xylem vulnerability curves, which describe the relationship between the percentage of loss of $k_{s\text{-max}}$ caused by embolism and stem xylem water potential (Ψ_{stem}); vulnerability curves were constructed using the centrifugal force technique (Alder *et al.* 1997). The centrifuge (Sorvall RC5C, Thermo Fisher Scientific, Waltham, MA, USA) had a custom-designed rotor holding 14.2-cm-long samples. Stems were spun to generate water potentials stepwise from -0.5 to -2 MPa. After each spin, hydraulic conductivity was remeasured to determine the percent loss of conductivity. After conductivity measurements were complete, stems were dried at 70 °C for dry mass.

Leaf vulnerability to embolism was measured by assessing rehydration kinetics in detached single, mature leaves from three trees per chamber (six trees per treatment), and determined as in Brodribb & Holbrook (2003):

$$K_{\text{leaf}} = C_{\text{leaf}} \ln[\Psi_{\text{leaf(o)}} / \Psi_{\text{leaf(t)}}] / t \quad (1)$$

where K_{leaf} ($\text{mmol m}^{-2} \text{MPa}^{-1} \text{s}^{-1}$) is the leaf hydraulic conductance, C_{leaf} ($\text{mmol m}^{-2} \text{MPa}^{-1}$) is the leaf capacitance, $\Psi_{\text{leaf(o)}}$ (MPa) is the leaf water potential prior to rehydration, $\Psi_{\text{leaf(t)}}$ is the leaf water potential after rehydration and t (s) is the duration of rehydration of leaves detached under water from the stem. C_{leaf} was determined from the slope of relative water content to Ψ_{leaf} obtained from leaf pressure–volume curves (P-V curves; Brodribb & Holbrook 2003). Values of K_{leaf} were corrected for a viscosity of water at a temperature of 20 °C.

Pressure–volume analyses (P-V curves; Tyree & Hammel 1972) were conducted on mature and fully expanded leaves taken from at least three seedlings per chamber. Samples were cut at the petiole base with a

razor blade early in the morning prior to significant water loss, and immediately submerged in water. After a minimum of 5 min, the leaf was blotted dry. P-V curves were initiated by determining leaf fresh weight and then measuring Ψ_{leaf} with a pressure chamber. Alternate determinations of fresh weight and Ψ_{leaf} were repeated during slow dehydration on the laboratory bench until Ψ_{leaf} was between -2.5 MPa to -3.0 MPa. The inverse of Ψ_{leaf} was plotted against relative water content to establish P-V curves and determine the turgor loss point (Ψ_{tp}) and C_{leaf} . For normalizing C_{leaf} on a leaf area basis, leaf areas were obtained with the leaf area meter.

Gas exchange and leaf biochemistry

We emphasized measurements of the photosynthetic parameters required by the Soil–Plant–Atmosphere model because the main focus of this study was on thermal acclimation of hydraulic traits and not photosynthesis (see below). Gas exchange was measured in the 13–14th weeks of growth, when AT seedlings had fully expanded leaves. Responses of net CO_2 assimilation rates (A_{net}) to changes in intercellular CO_2 concentrations (C_i) were measured on the 9–10th leaf from the stem top with a portable photosynthesis system (Li-Cor 6400, Li-Cor). Cuvette conditions were maintained at 25 °C, light levels of 1000 $\mu\text{mol photons m}^{-2} \text{s}^{-1}$ and a D of 1.7–1.8 kPa. CO_2 concentrations began at 400 $\mu\text{mol mol}^{-1}$, were lowered stepwise to 50 $\mu\text{mol mol}^{-1}$, reset to 400 $\mu\text{mol mol}^{-1}$ and then raised stepwise to 1500 $\mu\text{mol mol}^{-1}$; measurements were made once values were stable at the new CO_2 concentration. Gas exchange was measured on six seedlings from each chamber (total of $n = 12$ per treatment). Maximum rates of ribulose 1,5-bisphosphate carboxylase/oxygenase (Rubisco) carboxylation (V_{max}) and maximum electron transport rates (J_{max}) were calculated as per Farquhar, von Cammerer and Berry (1980), using the methods and parameters from Way & Sage (2008). After gas exchange measurements were completed, measured leaves were harvested, frozen in liquid N_2 and stored at -80 °C. Half of each leaf was dried and finely ground to determine leaf nitrogen and carbon content (Carlo-Erba NC2100 elemental analyzer, ThermoQuest Italia, Milan, Italy).

Three young, fully expanded leaves from each chamber were sampled from the final biomass harvest for carbon isotope analysis. Leaves were dried for 48 h at 70 °C and finely ground. The ^{13}C content of the bulk leaf, as well as the leaf carbon and nitrogen contents, was determined using a Carlo-Erba NA1500 elemental analyzer (ThermoQuest Italia) equipped with a Costech zero-blank autosampler (Costech Analytical Technologies Inc., Valencia, CA, USA). Resulting purified and chromatographically separated CO_2 were passed by continuous flow to a ThermoFinnigan Delta+XL IRMS via a ConFlo III interface (Thermo Fischer Scientific, West Palm Beach, FL, USA). The $\delta^{13}\text{C}$ was calculated by Isodat 3.0 software (Thermo Fischer Scientific), and was normalized and corrected to the international scale [Vienna Pee Dee belemnite (V-PDB)] using a suite of

calibrated internal standards. The ratio of standards to samples analysed was approximately 1:4.

Modelling

To predict the effect of high growth temperatures on plant water and carbon exchange, we used the SPA model that is designed to represent processes common to vascular plants (see details in Williams *et al.* 1996, 2001; Hill, Williams & Moncrieff 2008). SPA is a process-based model that simulates ecosystem photosynthesis, tree water use and stand water balance at fine temporal and spatial scales (30 min time step, multiple canopy and soil layers). In the model, the maximum flux rate of water through vegetation is determined by the difference between soil and leaf Ψ and is controlled by K_{plant} . Leaf-to-air energy, water and CO_2 exchange consists of a coupled photosynthesis model (Farquhar model) with a stomatal conductance model. The scale of parameterization (leaf level) and prediction (canopy level) have been designed to allow the model to diagnose eddy flux data, and to provide a tool for scaling up leaf level processes to canopy and landscape scales, but the basic physiological mechanisms are the same for seedlings and mature trees. For this study, we incorporated a stem cavitation function (Sperry *et al.* 1998). Our intent with this analysis was not to approximate a mature aspen stand, but instead to investigate how the coordinated changes in seedling growth and physiology might affect water and carbon fluxes over a larger scale (such as in young, regenerating aspen stands).

All of the allometric (leaf area index, root area index), hydraulic (K_{root} , K_{plant} , minimum leaf Ψ) and photosynthetic (J_{max} , V_{cmax} , leaf nitrogen content) input parameters used in the model were directly measured on seedlings and are presented throughout the results. Water and carbon fluxes were modelled using measured seedling characteristic such as height, diameter, leaf area index (LAI) and root area index (RAI). Peak LAI was $3.1 \text{ m}^2 \text{ m}^{-2}$ for AT and $4.4 \text{ m}^2 \text{ m}^{-2}$ for HT seedlings before senescence, and the ratio of RAI to LAI ranged from 5.1 for AT to 4.3 for HT poplars. Modelled LAI dynamics were assumed to follow a parabolic curve with leaf flush occurring on day 100 and peak LAI on day 225. Root biomass followed an exponential decrease with soil depth (Schenk & Jackson 2002), with 42% of the root biomass between 0 and 10 cm, 34% between 10 and 20 cm, 15% between 20 and 30 cm and 9% between 30 and 40 cm.

For the AT model scenario, we forced the SPA model with soil, meteorological and radiation data collected in 1996 at the Boreal-Ecosystem-Atmosphere-Study (BOREAS) old aspen (OAS) site (Osborne *et al.* 1998), the same site used to derive the AT experimental growth conditions. This year was chosen since it represents an average year for this region in terms of mean annual temperature (-3.6°C) and precipitation (460 mm per year). Seasonally, mean temperatures ranged from 16 to 27°C between June and August and from -20 to -30°C between November and February. Average precipitation in this region is low

(15–30 mm per month) from October to April, but increases sharply during the summer growing season (50–100 mm per month from June to August). Atmospheric CO_2 concentration was taken at 400 ppm to represent current ambient values and was representative of CO_2 levels in the phytotron over the course of the experiment (data not shown).

To determine how HT might alter seasonal carbon and water dynamics, we ran two additional model runs. Firstly, to isolate the effects of high growth temperatures on aspen morphology and physiology, we ran the model with the same AT environmental conditions, but used the measured HT seedling physiology (HT, current climate scenario). Lastly, to assess the combined impact of HT on seedling development and direct climate drivers, the HT physiological data was rerun with the same environmental data, but a 5°C increase air temperatures (HT, future climate scenario). For the HT scenario, all atmospheric conditions (light, wind speed, precipitation, relative humidity, CO_2) were kept the same as for the AT scenario except for temperature, although the increased air temperature also directly increased D in the HT climate scenario. Because the larger HT root mass may be able to explore deeper soils for water resources than AT roots, thereby offsetting potential increases in evaporative demand in a warmer climate, we also investigated the effect of increasing maximum rooting depth in HT seedlings in the HT climate scenario. Rooting depth was increased up to twofold, to match the approximately twofold greater root mass in HT than AT seedlings. The rooting depth sensitivity analysis maintained both the exponential decrease in root biomass with rooting depth and the HT root biomass value used in the other model scenarios.

Statistics

Significant differences in growth, biochemistry, photosynthesis and hydraulic traits between AT and HT seedlings were established using analyses of variance (ANOVAS) with chamber replicates nested in treatment using SAS 9.1 or JMP 8.0 (SAS, Cary, NC, USA).

RESULTS

Growth

Elevated growth temperatures significantly increased growth in aspen seedlings. HT seedlings were 26% taller, with 32% greater stem diameter, than AT seedlings by the end of the experiment (Fig. 1a; $P < 0.0001$ for both). All components of biomass were greater in HT than AT seedlings; total biomass was 59% higher, while leaf, stem and root masses increased 23, 111 and 68%, respectively, in high growth temperatures (Fig. 1b, $P < 0.05$ for all). There was also a trend for greater leaf area (a 40% increase) in HT seedlings (Table 2, $P = 0.08$), in keeping with their greater leaf mass.

Developmental trajectories of seedlings differed between temperature treatments. As seedlings grew, AT seedlings

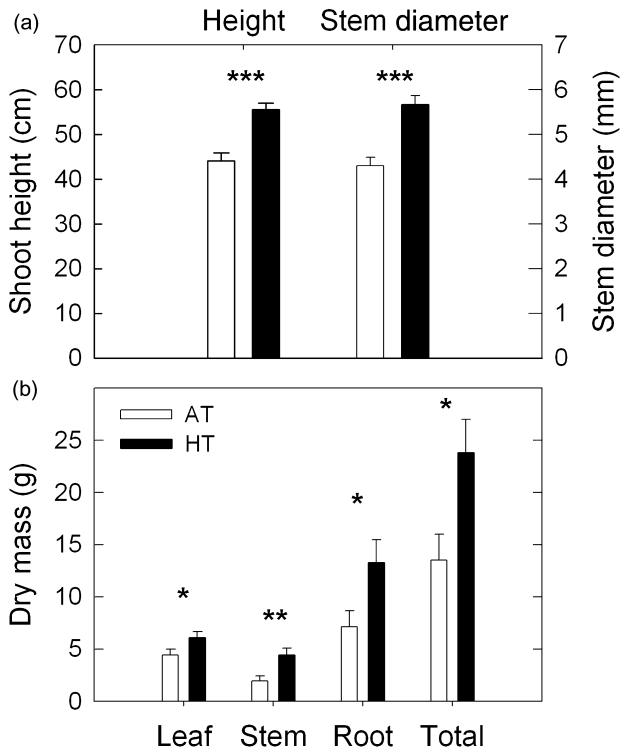


Figure 1. Growth of trembling aspen seedlings grown at either ambient (AT; empty bars) or high temperatures (HT, AT +5 °C; filled bars): (a) shoot height and stem diameter after 15 weeks of growth; (b) dry mass of seedlings and plant parts after 19 weeks of growth. Means \pm SE, $n = 58$ –71 for a; $n = 16$ –17 for b. * $P < 0.05$; ** $P < 0.001$; *** $P < 0.0001$.

put on more height per unit stem diameter growth than HT seedlings (Fig. 2a, $P < 0.038$), such that they became more slender than HT seedlings as they grew. Per unit biomass gain, HT seedlings gained less leaf mass and more root mass (Fig. 2b,d, $P = 0.0002$ for both). Seedlings from both treatments gained similar amounts of stem mass per unit biomass, but HT seedlings had greater stem mass than AT seedlings at all masses (Fig. 2c; $P < 0.0001$). There was no significant effect of temperature on the root:shoot ratio or

Table 2. Seedling and leaf morphological and biochemical traits for aspen seedlings grown under ambient (AT) or high temperatures (HT, AT +5 °C)

	AT	HT	<i>P</i> -value
Total leaf area (cm ²)	633.3 \pm 57.0	887.5 \pm 121.3	0.08
SLA (cm ² g ⁻¹)	202.1 \pm 14.5	229.3 \pm 27.7	<i>ns</i>
Leaf N (%)	1.59 \pm 0.06	1.74 \pm 0.06	0.06
$\delta^{13}\text{C}$ (‰)	-32.3 \pm 0.5	-29.6 \pm 0.8	<0.01
R/S	0.98 \pm 0.10	1.12 \pm 0.12	<i>ns</i>
LA/SA (cm ² cm ⁻²)	107.7 \pm 8.9	73.7 \pm 9.8	0.02

SLA, specific leaf area; leaf N, leaf nitrogen concentration; R/S, the root to shoot ratio; LA/SA, the ratio of leaf area to sapwood area.

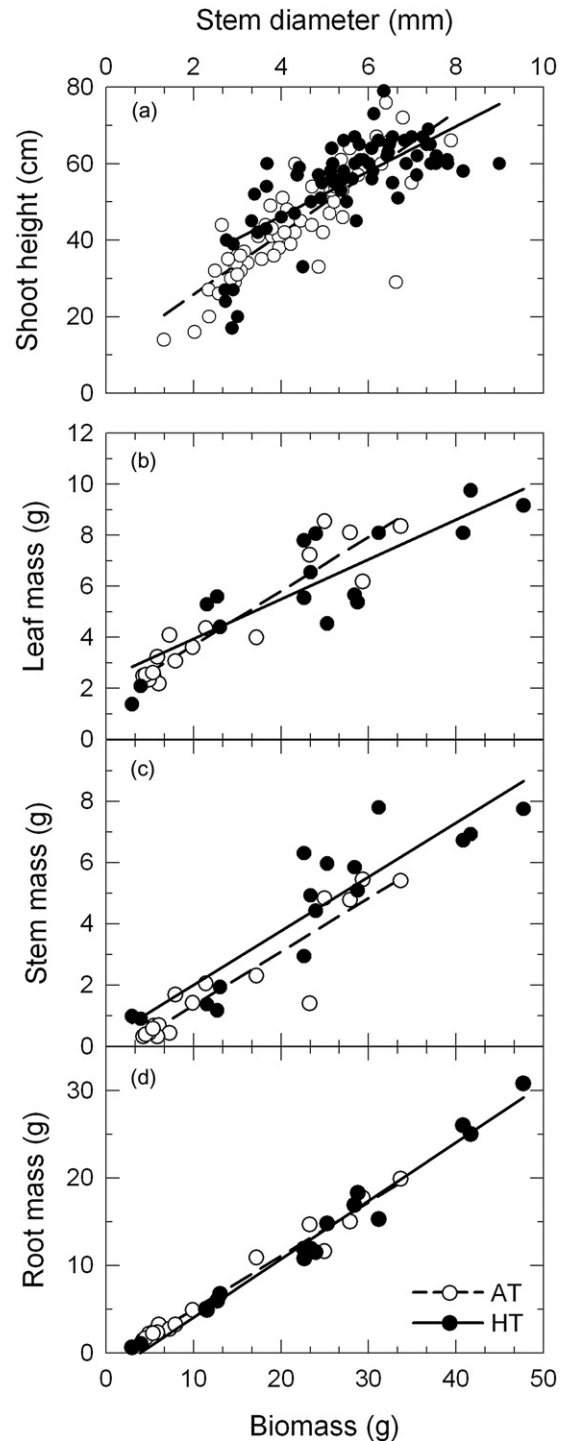


Figure 2. Growth of trembling aspen seedlings grown at either ambient (AT; empty symbols and dashed lines) or high temperatures (HT, AT +5 °C; filled symbols and solid lines): (a) shoot height and stem diameter after 15 weeks of growth; (b–d) dry mass of seedlings and plant parts after 19 weeks of growth.

on specific leaf area, but the ratio of leaf area to sapwood area (LA/SA) decreased by 31% ($P = 0.02$) in HT seedlings (Table 2).

Hydraulics

While the overall hydraulic conductance of the distal section comprising the newest 12 leaves of each leading stem ($K_{\text{tree-top}}$) was similar between temperature treatments (Table 3, $P > 0.05$), the partitioning of resistance between plant parts was significantly altered by growth temperature. In both treatments, most of the resistance to water flow of the distal section was in leaves (and specifically in the leaf laminae), but proportionally more of the resistance in the distal parts of HT seedlings was in stems and less in leaves compared to AT seedlings (Table 3). While partitioning of resistance within the distal section varied between growth temperatures, the top section of the tree provided a similar proportion of hydraulic conductance for the aboveground tree mass in both treatments (Table 3, $P = 0.90$).

Leaf hydraulic conductance (K_{leaf}) (leaf lamina + petiole) was 30% higher in HT than AT seedlings (Fig. 3a; $P = 0.02$) when measured with either the rehydration technique or the HPFM, and K_{leaf} decreased more rapidly with declining leaf water potential in HT than AT leaves (Supporting Information Fig. S1). Root hydraulic conductance (K_{root}) was greatly increased by high growth temperatures, such that K_{root} was 3.4 times greater in HT than AT seedlings on a leaf area basis, and 4.1 times greater on a root area basis (Fig. 3a; $P \leq 0.02$ for both). The specific hydraulic conductivity (k_s) of both the upper and lower stem sections were

similar across treatments ($P > 0.10$), but there was a trend for HT petioles to have greater k_s than AT petioles, with mean petiole k_s increasing more than twofold at HT (Fig. 3b; $P = 0.1$). Differences in K_{leaf} , K_{root} and k_s between treatments translated into a trend for HT poplar to have higher whole-tree conductance (K_{tree}) than AT seedlings (Table 3, $P = 0.08$). The majority of the resistance to water flow across the entire plant was in leaves in both AT and HT poplar, with a similar partitioning between leaf laminae and petioles (Table 3, $P > 0.05$ for all). However, HT seedlings had more of their total resistance in stems, and less in roots, than AT seedlings (Table 3, $P \leq 0.05$).

While high growth temperatures increased the vulnerability of leaves to water stress-induced cavitation ($P < 0.05$), they did not affect the vulnerability of stems ($P < 0.05$, Table 4). The AT leaves demonstrated a 50% loss of conductivity (Ψ_{50}) at a water potential 0.35 MPa more negative than HT leaves (Fig. 4a, Table 4). Seedlings in both treatments experienced well-watered growth conditions, but there was a trend for HT seedlings to have less negative predawn Ψ than AT seedlings (Table 4, $P = 0.06$). By midday, this trend was absent, such that HT leaves had similar Ψ_s as AT leaves (Table 4, $P = 0.39$), and there was no difference in midday stem Ψ between treatments ($P = 0.38$). We compared midday Ψ values (Table 4) and vulnerability curves (Fig. 4a,b) to determine whether leaves and stems were operating under conditions that would significantly reduce their conductivity. At midday Ψ values, AT leaves had less than 5% loss of conductivity, while HT leaves had lost 11% of their leaf conductivity (Fig. 4a); AT and HT stems had 35 and 42% losses of stem conductivity, respectively, at midday stem Ψ values (Fig. 4b). The leaf physiological characteristics derived from P-V curves indicated that there was a trend for HT leaves to have a more negative turgor loss Ψ than AT leaves and to have a higher osmotic potential ($P = 0.09$ and 0.07 , respectively), but there was no difference in leaf capacitance between treatments either before or after turgor loss (Table 4).

Table 3. Hydraulic conductance of upper stem and components ($K_{\text{tree-top}}$; above node 12), whole-plant hydraulic conductance (K_{tree}) and their partitioning, as well as aboveground hydraulic conductance ($K_{\text{tree-aboveground}}$) in poplar seedlings grown under ambient (AT) or high temperatures (HT, AT +5 °C)

	AT	HT	P-value
$K_{\text{tree-top}}$ (mmol m ⁻² s ⁻¹ MPa ⁻¹)	18 ± 4	17 ± 3	ns
Resistance in leaves (%)	79 ± 2	59 ± 6	0.01
Resistance in leaf lamina (%)	65 ± 4	50 ± 6	0.065
Resistance in petioles (%)	14 ± 2	8 ± 1	ns
Resistance in stem (%)	21 ± 2	41 ± 6	0.01
$K_{\text{tree-base}}/K_{\text{tree-top}}$	3.2 ± 0.6	3.1 ± 0.7	ns
K_{tree} (mmol m ⁻² s ⁻¹ MPa ⁻¹)	6.3 ± 0.9	9.2 ± 0.6	0.08
Resistance in leaves	38 ± 4	42 ± 6	ns
Resistance in leaf lamina (%)	32 ± 2	36 ± 6	ns
Resistance in petioles (%)	9 ± 2	6 ± 1	ns
Resistance in stem (%)	8 ± 3	28 ± 6	0.02
Resistance in roots (%)	54 ± 5	29 ± 6	0.01
$K_{\text{tree-aboveground}}$ (mmol m ⁻² s ⁻¹ MPa ⁻¹)	15.3 ± 2.2	13.0 ± 2.4	ns

Means ± SE, $n = 3-4$ seedlings per chamber, two chambers.

$K_{\text{tree-top}}/K_{\text{tree-base}}$, ratio of hydraulic conductance in top stem section to the basal stem section.

Gas exchange and leaf biochemistry

There was no difference in any gas exchange parameters measured at 25 °C between treatments, including estimates of net photosynthesis, stomatal conductance and the maximum carboxylation rate of Rubisco (Table 5; $0.34 < P < 0.91$). Leaf N concentration tended to be lower in AT than HT seedlings ($P = 0.06$; Table 2), and the $\delta^{13}\text{C}$ was more negative in AT seedlings than in HT aspen ($P < 0.01$; Table 2).

Modelling

When measured differences in seedling growth and physiology were modelled over a growing season, those differences had strong effects on aspen water use, gross primary productivity (GPP) and water-use efficiency (WUE). The physiological changes caused by high growth temperatures translated into a 35% increase in annual water use (from

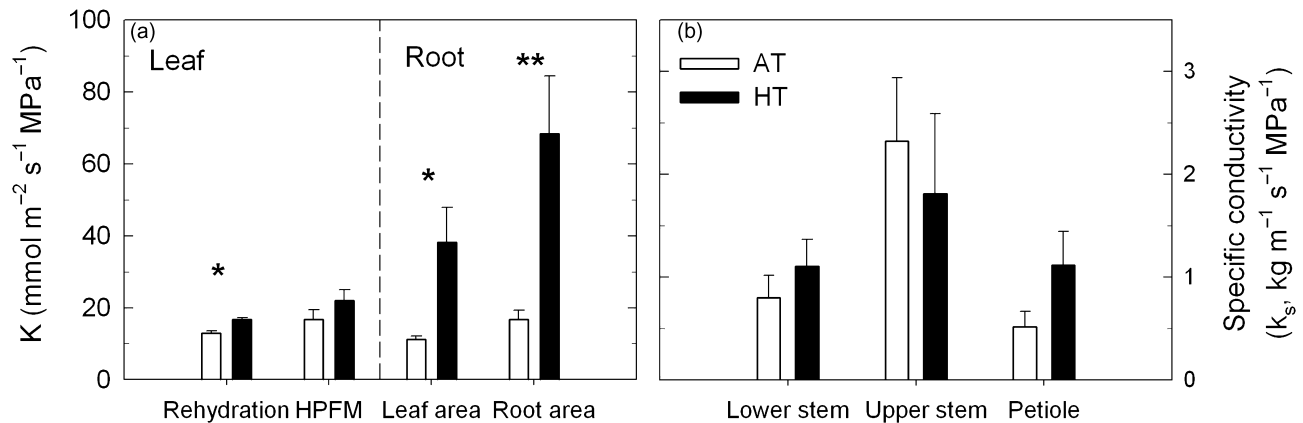


Figure 3. Hydraulic conductance (K) of (a) leaves (K_{leaf}) and roots (K_{root}), and (b) specific hydraulic conductivity (k_s) of petioles and upper and lower stems sections of trembling aspen seedlings grown at either ambient (AT) or high temperatures (HT, AT +5 °C). For comparison, K_{leaf} is given determined using the rehydration method and using the high-pressure flow meter (HPFM); K_{root} was determined on both a leaf area and root area basis. Means \pm SE, $n = 3\text{--}4$ seedlings per chamber, two chambers. * $P < 0.05$; ** $P < 0.001$; *** $P < 0.0001$.

278 to 374 $\text{kg H}_2\text{O year}^{-1}$) and a 23% increase in annual GPP (from 1056 to 1298 g C year^{-1}), when modelled for the current climate (Fig. 5a,b). When the direct impact of a 5 °C increase in air temperature (future climate) was added to the HT physiology scenario, high growth temperatures increased modelled annual GPP by 25% over ambient conditions (from 1056 to 1322 g C year^{-1}), but increased aspen water use 61% (from 278 to 448 $\text{kg H}_2\text{O year}^{-1}$; Fig. 5a,b). Sharp reductions in water use and GPP during the growing season in both HT scenarios were associated with strong, short-term declines in soil Ψ (Fig. 5c), with more negative soil Ψ s in the HT scenarios under a warmer climate than under current climate conditions. Increasing rooting depth in HT aspen did not erase these sudden decreases in water use or GPP (data not shown), although doubling rooting depth increased both by up to 15% (Supporting Information Table S1). The effect of the combined physiological and climate changes was a projected 35% reduction in WUE in modelled HT seedlings, regardless of the climate, compared to AT aspen at current climate conditions (Fig. 5d).

DISCUSSION

Some of the largest increases in temperature from climate change are predicted for high latitudes, such as the boreal forest (Christensen *et al.* 2007). While the extensive forests in this region play an important role in the global water and carbon cycles, few studies have explored how warmer growing temperatures may alter water transport and WUE in high-latitude tree species. We therefore studied the growth and hydraulic responses to HT in seedlings of a widely distributed boreal tree species, as well as modelling the potential water and carbon flux implications of our results. We found that high growth temperatures promoted seedling growth, but altered seedling allometry to promote allocation to roots over leaves as seedlings grew larger. With regard to hydraulics, there was a trend for greater water

transport capacity in seedlings that developed at warmer temperatures. Elevated growth temperatures also increased the drought vulnerability of leaves and induced significant shifts in seedling hydraulic architecture, altering the partitioning of hydraulic resistance within seedlings by reducing below-ground hydraulic resistance at the expense of above-ground resistance. Thus, while the greatest effects of warming air might be expected to be on aboveground tissues, root hydraulic traits in seedlings were more responsive to changes in temperature than leaves, with stem water transport capacity generally unaffected. Extending these results with a modelling approach demonstrated that while acclimation to high growth temperatures may increase aspen GPP, in our model scenarios, it stimulated water loss more, which could lead to more frequent severe drought stress in this system.

Our results support the finding that elevated temperatures increase growth in deciduous tree species, and that the growth of boreal tree species may be stimulated by warming when ample water and nutrient supplies are available (see review by Way & Oren 2010). However, the changes in growth trajectory in *P. tremuloides* shown here differ from those characterized in Way & Oren (2010), where elevated growth temperatures proportionally increased leaf mass and reduced root mass. Instead, we found a decrease in leaf mass and a slight increase in root mass per unit biomass gain in aspen grown at warmer temperatures, compared to ambient seedlings. These allocation changes could help increase water supply to the canopy, as could the lower ratio of leaf area to sapwood area in HT seedlings, which may be important in a warmer climate where the driving gradient (D) for transpiration is expected to increase. But extrapolating the effects of changes in biomass allocation into predictions for water transport or use assumes that hydraulic traits remain constant across growth temperatures, an assumption which was not supported by our data.

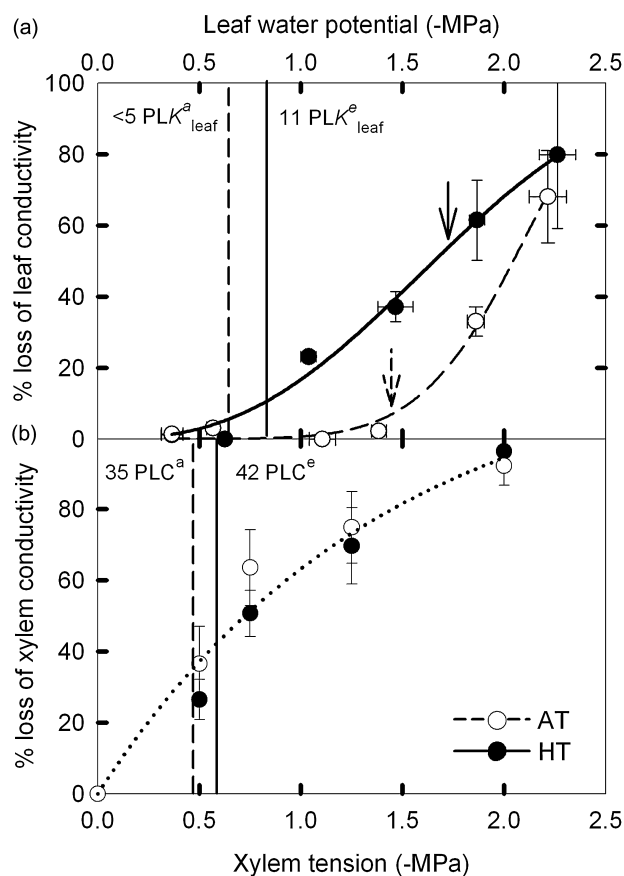


Figure 4. Percent loss of hydraulic conductivity versus water potential in (a) leaves and (b) stems of trembling aspen seedlings grown at either ambient (AT; empty symbols and dashed line) or high temperatures (HT, AT +5 °C; filled symbols and solid line). Dotted line in lower panel indicates combined response of AT and HT stems since there was no significant difference between treatments. Vertical dashed and solid lines indicate midday leaf and stem water potentials; arrows indicate leaf turgor loss points. Percent loss of conductivity for either leaf (PLK_{leaf}) or stems (PLC) under ambient or high temperature at measured leaf and stem water potentials are also given. Means ± SE, $n = 3-4$ seedlings per chamber, two chambers.

Thermal acclimation of hydraulic conductance

Separating the effects of ontogeny from treatment effects is important for determining whether physiological changes are driven directly by elevated growth temperatures, or indirectly through accelerated development (Tjoelker, Oleksyn & Reich 1998). To minimize ontogenetic effects, we compared hydraulic conductance in the stem section encompassing the 12 youngest leaves ($K_{\text{tree-top}}$), thus measuring similarly developed leaves, petioles and stems in both AT and HT poplars. Although $K_{\text{tree-top}}$ was similar between treatments, which could indicate that whole-plant conductance (K_{tree}) differences were due to accelerated HT growth, HT seedlings had a greater proportion of hydraulic resistance in stem tissue, both in the distal stem and in whole-plant measurements. Thus, even when developmental differences were accounted for, we found that growth

Table 4. Leaf and stem water potential (Ψ) values for aspen seedlings grown under ambient (AT) or high temperatures (HT, AT +5 °C)

	AT	HT	<i>P</i> -value
Predawn leaf Ψ (MPa)	-0.37 ± 0.03	-0.27 ± 0.03	0.06
Midday leaf Ψ (MPa)	-0.64 ± 0.04	-0.82 ± 0.07	<i>ns</i>
Midday stem Ψ (MPa)	-0.46 ± 0.02	-0.58 ± 0.04	<i>ns</i>
Leaf Ψ_{50} (MPa)	-2.01 ± 0.13	-1.66 ± 0.09	0.038
Stem Ψ_{50} (MPa)	-0.68 ± 0.14	-0.84 ± 0.13	<i>ns</i>
Turgor loss Ψ (MPa)	-1.45 ± 0.19	-1.76 ± 0.20	0.035
Osmotic potential at full hydration (Π , MPa)	-0.80 ± 0.13	-1.00 ± 0.17	0.07
Leaf capacitance before turgor loss ($\text{mmol m}^{-2} \text{MPa}^{-1}$)	738 ± 51	697 ± 52	<i>ns</i>
Leaf capacitance after turgor loss ($\text{mmol m}^{-2} \text{MPa}^{-1}$)	884 ± 152	933 ± 78	<i>ns</i>

Means ± SE, $n = 3-4$ seedlings per chamber, two chambers. Ψ_{50} , Ψ where 50% loss of conductivity occurs.

temperature altered seedling hydraulic structure. While some of these changes in hydraulic traits were proportionally large, the small sample size ($n = 2$ chambers) resulted in marginal significance for some parameters ($P \approx 0.1$); these results should be interpreted with caution and confirmed by future experiments.

The effects of high growth temperatures on K were most pronounced on the distal ends of the plant, producing a similar level of hydraulic resistance across plant organs by redistributing it away from roots and towards leaves. The overall trend was for HT seedlings to increase their root hydraulic capacity: K_{root} was more than threefold greater in HT than AT seedlings. The percentage of total plant hydraulic resistance accounted for by roots was decreased by high growth temperatures, but this was not caused by the larger root systems (and larger diameter roots) of HT seedlings since there was no relationship between root mass and

Table 5. Photosynthetic parameters for aspen seedlings grown under ambient (AT) or high temperatures (HT, AT +5 °C)

	Mean of AT and HT	<i>P</i> -value
A_{net} ($\mu\text{mol m}^{-2} \text{s}^{-1}$)	10.5 ± 0.5	<i>ns</i>
g_s ($\text{mol m}^{-2} \text{s}^{-1}$)	0.32 ± 0.03	<i>ns</i>
WUE_i ($\mu\text{mol mmol}^{-1}$)	2.53 ± 0.29	<i>ns</i>
V_{cmax} ($\mu\text{mol m}^{-2} \text{s}^{-1}$)	41.8 ± 2.2	<i>ns</i>
J_{max} ($\mu\text{mol m}^{-2} \text{s}^{-1}$)	64.6 ± 3.0	<i>ns</i>

There were no significant differences between treatments (*ns*, non-significant). Values are the means ± SE of both AT and HT seedlings ($n = 6$ seedlings per chamber, four chambers, 24 seedlings total).

A_{net} , net photosynthetic rate; g_s , stomatal conductance rate; WUE_i , instantaneous water-use efficiency (A_{net} divided by transpiration rate); V_{cmax} , maximum carboxylation rate of Rubisco; J_{max} , maximum electron transport rate.

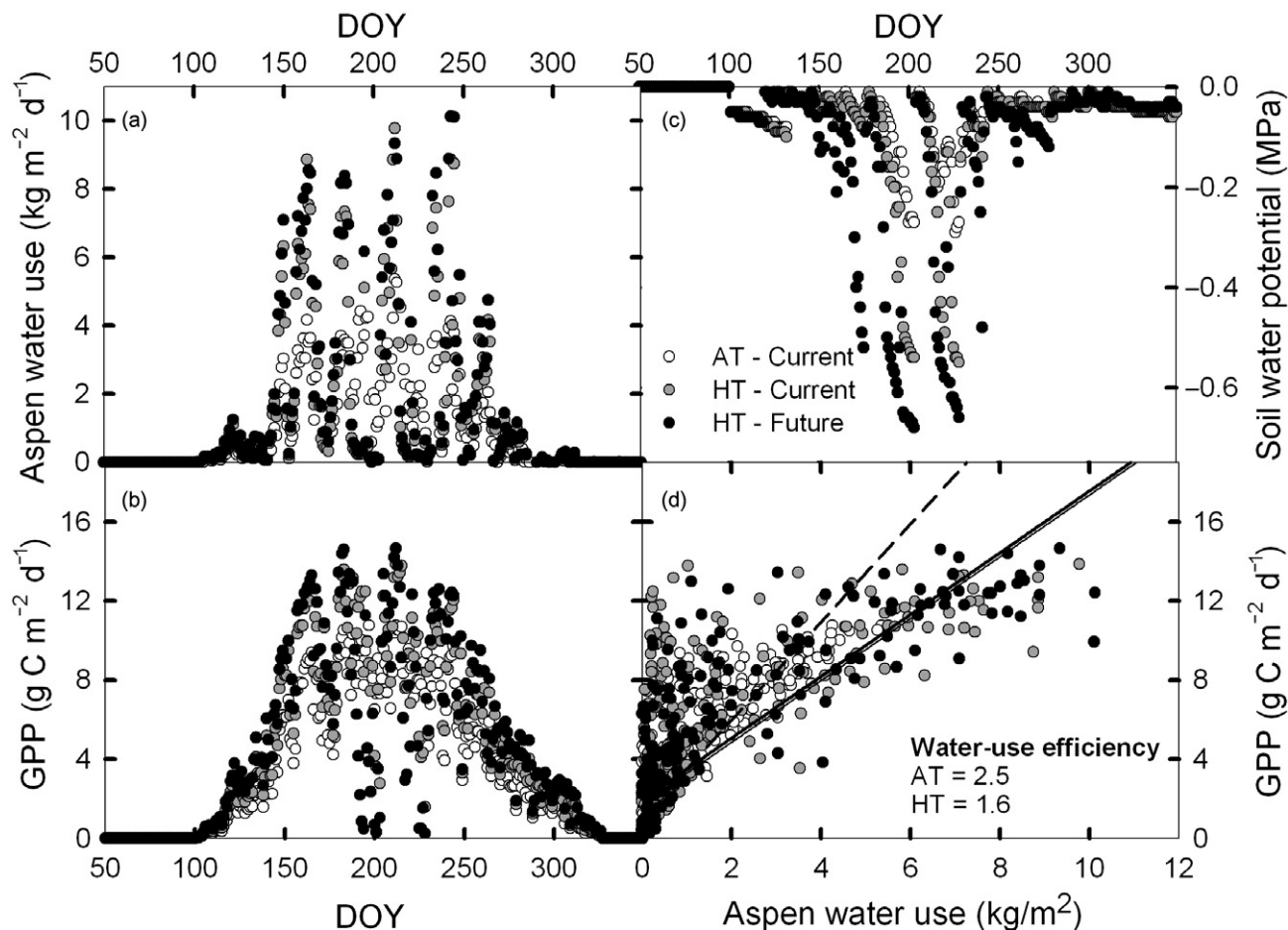


Figure 5. Modelled daily water and carbon fluxes per unit ground surface area for aspen with ambient temperatures (AT) seedling physiology at current climate (empty symbols), high temperatures (HT) seedling physiology at current climate (grey symbols), and HT seedling physiology at a future, 5 °C warmer climate (black symbols). (a) Modelled aspen water use; (b) modelled gross primary productivity (GPP); (c) modelled soil water potential; (d) modelled water-use efficiency, estimated as the slope of GPP versus aspen water use.

the percent root resistance ($P = 0.43$, $r^2 = 0.06$, data not shown). The greater K_{root} in HT seedlings increased the percent of total resistance attributable to stem tissue, although K_{stem} was unaffected by growth temperatures. The increase in HT K_{root} also shifted hydraulic resistance towards leaves, such that leaves constituted the largest resistance to water flow in HT seedlings on both an above-ground and whole-plant basis, while roots provided the majority of resistance in AT seedlings.

Vulnerability to cavitation

There is often assumed to be a trade-off between xylem efficiency and safety, involving a balance between maximizing hydraulic conductance through increasing vessel diameter and pit membrane porosity and maximizing safety from cavitation through reducing these traits (Zimmermann 1983), although the evidence for such a trade-off is equivocal (Maherali, Pockman & Jackson 2004). Using two different methods, we showed that HT leaves had 40% higher K_{leaf} than AT leaves, with the difference in absolute

values of K_{leaf} likely caused by methodological differences (Blackman & Brodribb 2011). This greater hydraulic conductance of HT than AT leaves may correspond to greater vulnerability to air-seeding embolism and to cavitation at less negative leaf Ψ values. Indeed, leaves from HT seedlings showed a greater loss of conductivity than AT leaves at the same leaf Ψ . Despite being more vulnerable to water stress-induced embolism, HT leaves operated at more negative leaf Ψ s and lost turgor at a more negative leaf Ψ than AT leaves. And while HT leaves showed greater losses of hydraulic conductivity at midday Ψ than AT leaves, both treatments had a similar operational K_{leaf} at their midday Ψ when assessed with leaf vulnerability curves.

In contrast to the strong differences in leaf hydraulic traits, AT and HT stems were equally vulnerable to cavitation as water stress developed. Stems reached a 50% loss of conductivity at very high Ψ s (−0.76 MPa across the treatments), consistent with studies in other *Populus* species (Hacke *et al.* 2011). Because of this extremely vulnerable stem xylem, stems in both treatments had large losses of conductivity at midday stem Ψ , despite being well watered.

Other studies have found considerable proportions of xylem embolism in *Populus* species during the growing season: in *P. fremontii* stems, 27–35% of xylem had native embolism (Leffler, England & Naito 2000), twigs of *P. tremuloides* had >50% embolized xylem at stem Ψ s of -0.9 to -1.2 MPa (Sperry *et al.* 1994) and *P. trichocarpa* also lost over 80% conductance at a stem Ψ of -1.25 MPa (Secchi & Zwieniecki 2011).

The high vulnerability to stem cavitation may underlie another surprising result in the data. Leaves are usually less resistant to cavitation than stems (Johnson *et al.* 2011), ensuring that embolisms damage the less costly and more easily replaced leaves before affecting stems. However, we found that stems from both temperature treatments were more vulnerable to cavitation than leaves, consistent with earlier work on *P. balsamifera* where stems lost 50% of their hydraulic conductivity at less negative Ψ s than petioles (Hacke & Sauter 1996). While we cannot explain why poplar stems are more vulnerable to cavitation than leaves, we can address some possibilities. Firstly, the discrepancy between leaves and stems may reflect the well-watered conditions of the experiment, where leaf Ψ remains high, in contrast with typical field conditions. To assess this, we used leaf and stem vulnerability curves and daily leaf and stem Ψ measured on seedlings and used Ψ predicted by the SPA model to estimate the seasonal percent loss of conductivity in both organs. In modelled AT aspen, leaves rarely lose more than 10% of their hydraulic conductivity, while stems lose 50–60% of their conductivity during the summer (Fig. 6a). Modelled HT seedlings operated at higher average losses of conductivity than AT aspen, and while HT leaves retained more than 90% of their maximum conductivity for over half the growing season, HT stems operated in this state for only 20% of the year (Fig. 6b). In both treatments, leaves still lose less conductivity than stems, and our results are unlikely to be due to measurement conditions. A second hypothesis is that if poplars depend on daily refilling of stem xylem and this incurs little cost, it may be easier to repair embolisms in stems than leaves, thus explaining why leaves are ‘overbuilt’ in terms of safety compared to stems. Secchi & Zwieniecki (2010) found diurnal losses of stem conductivity in well-watered *P. trichocarpa*, with full recovery by early evening, indicating that even under non-stressful conditions, poplars embolize and refill stem xylem daily. However, diurnal patterns of leaf hydraulic conductivity dynamics remain to be studied.

Carbon and water trade-offs

There was little evidence for thermal acclimation of photosynthetic capacity, consistent with a recent meta-analysis in trees (Way & Oren 2010). Despite the similarity in A_{net} measured at 25 °C, warmer temperatures likely stimulated A_{net} at growth conditions in HT aspen compared to AT seedlings since photosynthesis generally increases with rising temperature below the thermal optimum of 25–30 °C in C_3 species (Sage & Kubien 2007). Higher A_{net} in HT

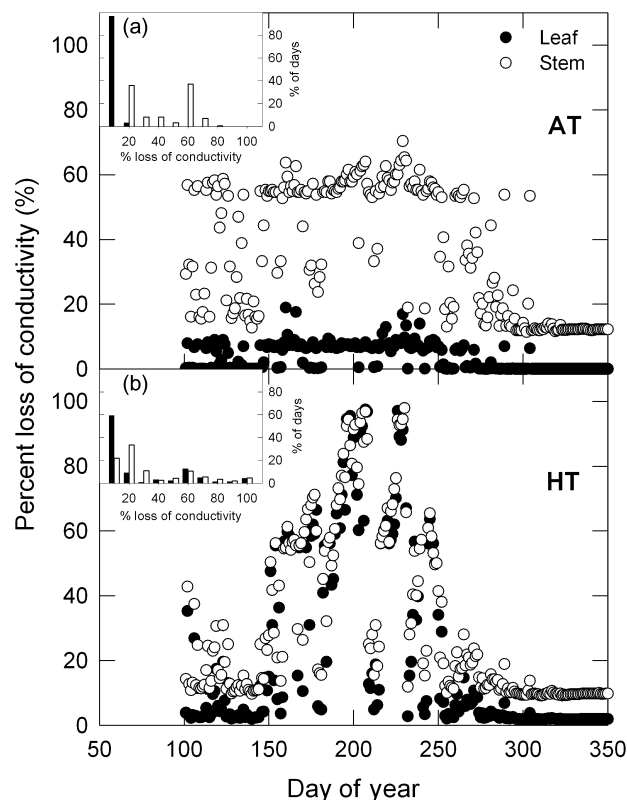


Figure 6. Modelled daily loss of hydraulic conductivity in leaves (filled symbols) and stems (empty symbols) over a growing season in trembling aspen seedlings grown at either (a) ambient temperatures (AT) or (b) high temperatures (HT, AT +5 °C). Insets show the frequency of growing season days with a given 10% bin of percent loss conductivity.

aspen would account for the larger size of HT seedlings, and is also supported by their higher $\delta^{13}\text{C}$ values, which indicate greater long-term leaf WUE than AT seedlings. Since there was no difference in WUE_i (A_{net}/E) at common measurement conditions, increased long-term WUE is attributable to differences in growth environment, rather than acclimation of either A_{net} or g_s . Higher D in the HT chambers would also lower g_s and increase WUE, thus the increased long-term WUE in HT trees was likely due to a combination of increased A_{net} and decreased g_s in the growth chambers.

While our goal was to compare the potential effects of physiological differences between AT and HT aspen on seasonal seedling water and carbon use, we also compared the AT seedling model results with measured stand-level water use at the BOREAS aspen site to gauge the model's performance. Modelled seasonal patterns and maximum rates of tree water use in the AT seedling scenario are similar to sap-flux measurements at the BOREAS aspen site for the year used to drive the SPA model (Hogg *et al.* 1997). Since the BOREAS site and our AT seedlings had similar LAI values, this provides some confidence that the measured seedling traits can be modelled realistically. We therefore compared the AT model outputs with those based on HT seedling measurements and the same environment,

or the same climate with a +5 °C temperature increase to reflect warmer growth conditions. While this analysis cannot make exact predictions of stand-level responses to warming, it does produce insights into how the suite of physiological changes measured in HT seedlings may impact larger scale ecological phenomena.

Both annual aspen water use and GPP were greater in HT scenarios compared to modelled AT seedlings. But since GPP was stimulated less than water use, high growth temperatures reduced WUE, regardless of the climate used in the model. The physiological and morphological acclimation of aspen to high growth temperatures caused most of the increase in modelled GPP since both HT scenarios had similar increases in annual GPP, despite different modelled climates. In contrast, there was an additive effect of physiology and climate on aspen water use in the HT scenarios. Under current climate conditions, physiological differences between AT and HT seedlings increased water use 35% in modelled HT aspen, but increasing air temperatures to reflect potential future climate warming increased water use a further 20%.

The modelled HT seedlings showed extreme fluctuations in water and carbon fluxes during the growing season, in comparison to the AT scenario. These rapid fluctuations were due to a depletion of soil water that reduced leaf Ψ below the turgor loss point, inducing stomatal closure in modelled HT aspen and could not be erased by as much as a doubling of rooting depth to access deeper soil water. This severe drought stress occurred despite using the same precipitation drivers in both AT and HT stands. If precipitation is reduced, as might occur with climate change, these declines in stand transpiration would occur more frequently, and for longer periods, thus further reducing both GPP and water use. As seen by the low stem Ψ_{50} for this species, such an increase in drought frequency or severity could put these trees at risk of total hydraulic failure and death (Anderegg *et al.* 2012).

ACKNOWLEDGMENTS

We would like to thank Will Cook, Mark Sherrard and the Duke Phytotron staff for their assistance in germination and plant care, and Dan Johnson for stimulating discussions. Seeds for this experiment were generously supplied by the Canadian National Tree Seed Centre. Way was supported by an NSERC fellowship, the U.S. Department of Agriculture (2011-67003-30222), and the Department of Energy's Biological and Environmental Research, Terrestrial Ecosystem Sciences program (11-DE-SC-0006967). Support for the experiment came from the southeastern region of the DOE-funded National Institute for Climate Change Research. R.B.J. acknowledges support from the Department of Energy's National Institute for Climate Change research, southeastern region. J.C.D. acknowledges support from the Department of Energy's Biological and Environmental Research, Terrestrial Ecosystem Sciences program (11-DE-SC-0006700).

REFERENCES

- Alder N.N., Pockman W.T., Sperry J.S. & Nuismer S. (1997) Use of centrifugal force in the study of xylem cavitation. *Journal of Experimental Botany* **48**, 665–674.
- Anderegg W.R.L., Berry J.A., Smith D.D., Sperry J.S., Anderegg L.D.L. & Field C.B. (2012) The roles of hydraulic and carbon stress in a wide spread climate-induced forest die-off. *Proceedings of the National Academy of Sciences of the United States of America* **109**, 233–237.
- Blackman C.J. & Brodribb T.J. (2011) Two measures of leaf capacitance: insights into the water transport pathway and hydraulic conductance in leaves. *Functional Plant Biology* **38**, 118–126.
- Brodribb T.J. & Holbrook N.M. (2003) Stomatal closure during leaf dehydration, correlation with other leaf physiological traits. *Plant Physiology* **132**, 2166–2173.
- Christensen J.H., Hewitson B., Busuioc A., *et al.* (2007) Regional climate projections. In *Climate Change 2007: The Physical Science Basis. Contribution of Working Group I to the Fourth Assessment Report of the Intergovernmental Panel on Climate Change* (eds S. Solomon, D. Qin, M. Manning, Z. Chen, M. Marquis, K.B. Averyt, M. Tignor & H.L. Miller), pp. 847–940. Cambridge University Press, Cambridge, UK and New York, NY, USA.
- Domec J.-C., Palmroth S., Ward E., Maier C.A., Thereuzien M. & Oren R. (2009) Interactive effects of long term elevated CO₂ and N-fertilization on the coordination between leaf hydraulic conductance and stomatal conductance in *Pinus taeda*. *Plant, Cell & Environment* **32**, 1500–1512.
- Farquhar G.D. & Sharkey T.D. (1982) Stomatal conductance and photosynthesis. *Annual Review of Plant Physiology* **33**, 317–345.
- Farquhar G.D., von Cammerer S. & Berry J.A. (1980) A biochemical model of photosynthetic CO₂ assimilation in leaves of C3 plants. *Planta* **149**, 78–90.
- Givnish T.J. (ed.) (1986) *On the Economy of Plant Form and Function*. Cambridge University Press, Cambridge, UK.
- Hacke U. & Sauter J.J. (1996) Drought-induced xylem dysfunction in petioles, branches, and roots of *Populus balsamifera* L. and *Alnus glutinosa* (L.) Gaertn. *Plant Physiology* **111**, 413–417.
- Hacke U.G., Plavcová L., Almeida-Rodriguez A., King-Jones S., Zhou W. & Cooke J.E.K. (2011) Influence of nitrogen fertilization on xylem traits and aquaporin expression in stems of hybrid poplar. *Tree Physiology* **30**, 1016–1025.
- Hill T.C., Williams M. & Moncrieff J.B. (2008) Modeling feedbacks between a boreal forest and the planetary boundary layer. *Journal of Geophysical Research* **113**, D15122. doi:10.1029/2007JD009412.
- Hogg E.H., Black T.A., den Hartog G., *et al.* (1997) A comparison of sap flow and eddy fluxes of water vapor from a deciduous boreal forest. *Journal of Geophysical Research* **102**, 28929–28937.
- Johnson D.M., McCulloh K.A., Meinzer F.C., Woodruff D.R. & Eissenstat D.M. (2011) Hydraulic patterns and safety margins, from stem to stomata, in three eastern US tree species. *Tree Physiology* **31**, 659–668.
- Kumagai T., Katul G.G., Porporato A., Saitoh S., Ohashi M., Ichie T. & Suzuki M. (2004) Carbon and water cycling in a Bornean tropical rainforest under current and future climate scenarios. *Advances in Water Resources* **27**, 135–150.
- Leffler A.J., England L.E. & Naito J. (2000) Vulnerability of Fremont cottonwood (*Populus fremontii* Wats.) individuals to xylem cavitation. *Western North American Naturalist* **60**, 204–210.
- Maherali H. & DeLucia E.H. (2000a) Xylem conductivity and vulnerability to cavitation of ponderosa pine growing in contrasting climates. *Tree Physiology* **20**, 859–867.

- Maherali H. & DeLucia E.H. (2000b) Interactive effects of elevated CO₂ and temperature on water transport in ponderosa pine. *American Journal of Botany* **87**, 243–249.
- Maherali H., Pockman W.T. & Jackson R.B. (2004) Adaptive variation in the vulnerability of woody plants to xylem cavitation. *Ecology* **85**, 2184–2199.
- Meinzer F.C. (2002) Co-ordination of vapour and liquid phase water transport properties in plants. *Plant, Cell & Environment* **25**, 265–274.
- Osborne H., Young K., Wittrock V. & Shewchuck S. (1998) BOREAS/SRC AMS Suite A Surface Meteorological and Radiation Data: 1996. Data set. Available online [http://www.daac.ornl.gov] from Oak Ridge National Laboratory Distributed Active Archive Center, Oak Ridge, TN, USA. doi:10.3334/ORNLDAAC/464.
- Perala D.A. (1990) *Populus tremuloides* Michx. In *Silvics of North America, Vol. 2 Hardwoods*. Agriculture Handbook 654 (eds R.M. Burns & B.H. Honkala), pp. 559–569. United States Department of Agriculture, Forest Service, Washington, DC, USA.
- Phillips N.G., Attard R.D., Ghannoum O., Lewis J.D., Logan B.A. & Tissue D.T. (2011) Impact of variable [CO₂] and temperature on water transport structure-function relationships in *Eucalyptus*. *Tree Physiology* **31**, 945–952.
- Sack L., Melcher P.J., Zwieniecki M.A. & Holbrook N.M. (2002) The hydraulic conductance of the angiosperm leaf lamina: a comparison of three measurement methods. *Journal of Experimental Botany* **53**, 2177–2184.
- Sage R.F. & Kubien D.S. (2007) The temperature response of C₃ and C₄ photosynthesis. *Plant, Cell & Environment* **30**, 1086–1106.
- Schenk H.J. & Jackson R.B. (2002) Rooting depths, lateral spreads, and below-ground/aboveground allometries of plants in water-limited ecosystems. *Journal of Ecology* **90**, 480–494.
- Secchi F. & Zwieniecki M.A. (2010) Patterns of PIP gene expression in *Populus trichocarpa* during recovery from xylem embolism suggest a major role for the PIP1 aquaporin subfamily as moderators of refilling process. *Plant, Cell & Environment* **33**, 1285–1297.
- Secchi F. & Zwieniecki M.A. (2011) Sensing embolism in xylem vessels: the role of sucrose as a trigger for refilling. *Plant, Cell & Environment* **34**, 514–524.
- Sperry J.S., Nichols K.L., Sullivan J.E.M. & Eastlack S.E. (1994) Xylem embolism in ring-porous, diffuse-porous, and coniferous trees of northern Utah and interior Alaska. *Ecology* **75**, 1736–1752.
- Sperry J.S., Adler F.R., Campbell G.S. & Comstock J.P. (1998) Limitation of plant water use by rhizosphere and xylem conductance: results from a model. *Plant, Cell & Environment* **21**, 347–359.
- Thomas D.S., Montagu K.D. & Conroy J.P. (2004) Changes in wood density of *Eucalyptus camaldulensis* due to temperature – the physiological link between water viscosity and wood anatomy. *Forest Ecology and Management* **193**, 157–165.
- Tjoelker M.G., Oleksyn J. & Reich P.B. (1998) Seedlings of five boreal tree species differ in acclimation of net photosynthesis to elevated CO₂ and temperature. *Tree Physiology* **18**, 715–726.
- Trenberth K.E., Fasullo J. & Smith L. (2005) Trends and variability in column-integrated water vapor. *Climate Dynamics* **24**, 741–758.
- Tyree M.T. & Hammel H.T. (1972) The measurement of the turgor pressure and the water relations of plants by the pressure-bomb technique. *Journal of Experimental Botany* **23**, 267–282.
- Tyree M.T. & Sperry J.S. (1988) Do woody plants operate near the point of catastrophic xylem dysfunction caused by dynamic water stress? Answers from a model. *Plant Physiology* **88**, 574–580.
- Tyree M.T., Sinclair B., Lu P. & Granier A. (1993) Whole shoot hydraulic resistance in *Quercus* species measured with a new high pressure flowmeter. *Annals of Forest Science* **50**, 417–423.
- Tyree M.T., Nardini A., Salleo S., Sack L. & El Omari B. (2005) The dependence of leaf hydraulic conductance on irradiance during HPFM measurements: any role for stomatal response? *Journal of Experimental Botany* **56**, 737–744.
- Voicu M.C. & Zwiazek J.J. (2010) Inhibitor studies of leaf lamina hydraulic conductance in trembling aspen (*Populus tremuloides* Michx.) leaves. *Tree Physiology* **30**, 193–204.
- Way D.A. & Oren R. (2010) Differential responses to increased growth temperatures between trees from different functional groups and biomes: a review and synthesis of data. *Tree Physiology* **30**, 669–688.
- Way D.A. & Sage R.F. (2008) Elevated growth temperatures reduce the carbon gain of black spruce (*Picea mariana* (Mill.) B.S.P.). *Global Change Biology* **14**, 624–636.
- Williams M., Rastetter E.B., Fernandes D.N., Goulden M.L., Wofsy S.C., Shaver G.R., Melillo J.M., Munger J.W., Fan S.-M. & Nadelhoffer K.J. (1996) Modelling the soil-plant-atmosphere continuum in a *Quercus-Acer* stand at Harvard Forest: the regulation of stomatal conductance by light, nitrogen and soil/plant hydraulic properties. *Plant, Cell & Environment* **19**, 911–927.
- Williams M., Law B.E., Anthoni P.M. & Unsworth M. (2001) Using a simulation model and ecosystem flux data to examine carbon-water interactions in ponderosa pine. *Tree Physiology* **21**, 287–298.
- Zimmermann M.H. (1983) *Xylem Structure and the Ascent of Sap*. Springer-Verlag, Berlin, Germany.

Received 22 February 2012; accepted for publication 7 June 2012

SUPPORTING INFORMATION

Additional Supporting Information may be found in the online version of this article:

Figure S1. Hydraulic conductance of leaves (K_{leaf}) versus water potential trembling aspen seedlings grown at either ambient (AT; empty symbols and dashed line) or high temperatures (HT, AT +5°C; filled symbols and solid line). Different symbol shapes indicate different individual leaves. Vertical lines indicate midday leaf water potentials; arrows indicate leaf turgor loss points.

Table S1. The effect of rooting depth on aspen tree water use, gross primary productivity (GPP) and water use efficiency for trees grown under high temperatures (HT). Modeling outputs in Fig. 5 assumed that while HT doubled root biomass, a maximum rooting depth of 40 cm was achieved for both ambient and HT aspen (see Material and Methods). For the data in Supporting Information Table S1, we used measured HT root biomass, following an exponential decrease with soil depth (Schenk & Jackson 2002), consistent with the methods used to generate Fig. 5.

Please note: Wiley-Blackwell are not responsible for the content or functionality of any supporting materials supplied by the authors. Any queries (other than missing material) should be directed to the corresponding author for the article.